JOURNAL OF MAGNETIC RESONANCE **128,** 149–160 (1997)
ARTICLE NO. MN971230

Off-Resonance Irradiation Effect in Steady-State NMR Saturation Transfer

Evelyne Baguet† and Claude Roby*

**Laboratoire de Résonance Magnétique en Biologie Métabolique, CEA and Université Joseph Fourier, 17 rue des Martyrs, 38054 Grenoble cedex 9, France; and †Laboratoire d'analyse isotopique et électrochimique de métabolismes, CNRS UPRES-A 6006, Université de Nantes, 2 rue de la Houssinière, F-44322 Nantes cedex 3, France*

Received August 22, 1994; revised July 21, 1997

The off-resonance irradiation effect (spill-over effect), occurring in steady-state NMR saturation-transfer experiments, is studied theoretically and experimentally for a two-spin system in chemical exchange, when a contralateral irradiation is applied to record the reference spectrum. The relevant parameter chosen for this study is the saturation-transfer ratio. It is defined as the ratio between the value of one exchanging magnetization, obtained when saturating the other, and that of the same magnetization measured when applying a contralateral irradiation. The theoretical study is carried out via a model based on the Bloch equations modified for chemical exchange and expressed in a doubly tilted single rotating frame. The saturation-transfer ratio is expressed as a function of the saturating RF field magnitude. It is shown that the RF field applied off-resonance during the acquisition of the reference spectrum does not correct the experimental saturation-transfer ratio for the spill-over effect. In fact, the saturation-transfer ratio increases with the magnitude of this field. This result is qualitatively explained by the consequence of the effective magnetic fields' relative orientations upon the amount of exchanged magnetization. The validity of the theoretical description is tested experimentally with a solution of *N,N*-dimethylacetamide in which chemical exchange arises from internal hindered rotation. An experimental protocol is proposed to detect spill-over and correct it when necessary. The way to describe spill-over theoretically when more than two spins interact by chemical exchange and/or dipolar coupling is also given.

INTRODUCTION

NMR saturation-transfer methods (*1, 2*) permit the study of chemical exchange and cross relaxation between nuclear spins. They are among the many NMR methods used in chemistry to study the structure and dynamics of molecules (*3, 4*). In biological systems, they are employed for the direct characterization of enzymatic reactions and transport properties in living cells (*5–7*).

The steady-state saturation-transfer technique, when coupled to relaxation rate measurements, is the most precise of the magnetization-transfer methods to measure unidirectional reaction rates of systems with a poor signal/noise ratio. When two populations are in exchange, this measurement is achieved by determining the longitudinal relaxation rate constant and the steady-state attenuation of one population's magnetization when the other is selectively saturated. Two major potential artifacts of such an experiment have already been studied: the modification of the longitudinal relaxation rate by off-resonance irradiation (*8*), and an incomplete saturation of the peak on resonance (*9*). In the case where saturation of this peak is complete, it has generally been assumed that the spill-over effect occurring during the steady-state saturation-transfer experiment can be corrected by the application of a ''contralateral irradiation'' when recording the reference spectrum (*10–14*). It has already been shown that this experimental protocol does not lead to the expected saturation-transfer ratio if the power envelope of the radiofrequency field used for saturation is not a symmetrical function of frequency (*15*). To date, no general study of the spill-over effect in steady-state saturation-transfer experiments has been reported.

Our aim is to evaluate the spill-over effect in steady-state NMR saturation-transfer experiments. For the sake of simplicity, the following presentation refers only to chemical exchange. The slight modifications of the model in the case of dipolar coupling are given in the Appendix.

THEORY

Chemical Exchange in a Two-Spin System

We consider a sample in which the nuclei, of gyromagnetic ratio γ, occupy alternatively two different chemical sites. At any time, the sample is composed of two populations A and B, giving rise to two different resonances. It is assumed that there is no chemical exchange nor dipolar interactions of A and B with other nuclei. The chemical exchange process, which is a transfer of matter, is coupled to an exchange of magnetization. As these two exchange phenomena have the same origin, they are characterized by the same unidirectional rate constants k_A and k_B of interconversion between populations A and B. They are usually represented by the scheme

1090-7807/97 $25.00

$$\mathrm{A} \underset{k_B}{\overset{k_A}{\rightleftharpoons}} \mathrm{B}.$$

This dynamic process can also be characterized by the time constants $\tau_A = 1/k_A$ and $\tau_B = 1/k_B$. The magnetization values of the two populations A and B at thermodynamic equilibrium are M_0^A and M_0^B respectively; their resonance angular frequencies are called ω_A and ω_B. If T_{1A} and T_{2A} are the relaxation times of A in the absence of exchange, it is appropriate to define the constants τ_{1A} and τ_{2A}

$$\frac{1}{\tau_{1A}} = \frac{1}{T_{1A}} + \frac{1}{\tau_A} \quad \text{and} \quad \frac{1}{\tau_{2A}} = \frac{1}{T_{2A}} + \frac{1}{\tau_A} \qquad [1]$$

and the same for B.

The magnetic properties of the spin system submitted to a RF field $\mathbf{B}_1$ of angular frequency ω_r and amplitude $B_1 = |\omega_1/\gamma|$ are transposed in the frame (x, y, z), rotating at angular frequency ω_r around the vertical axis, common to $\mathbf{B}_0$ and the z axis. The x axis shares the direction and orientation of the field $\mathbf{B}_1 = B_1\mathbf{e}_x$.

The magnetization components of A and B in this rotating frame are M_x^A, M_y^A, M_z^A, and M_x^B, M_y^B, M_z^B. Their dynamic properties are described by the Bloch equations modified for chemical exchange (*16*)

$$\frac{d}{dt} M_x^A = -\frac{M_x^A}{\tau_{2A}} - \Delta\omega_A M_y^A + \frac{M_x^B}{\tau_B} \qquad [2]$$

$$\frac{d}{dt} M_y^A = \Delta\omega_A M_x^A - \frac{M_y^A}{\tau_{2A}} + \frac{M_y^B}{\tau_B} - \omega_1 M_z^A \qquad [3]$$

$$\frac{d}{dt} M_z^A = \omega_1 M_y^A - \frac{M_z^A}{\tau_{1A}} + \frac{M_z^B}{\tau_B} + \frac{M_0^A}{T_{1A}}, \qquad [4]$$

where $\Delta\omega_A = \omega_A - \omega_r$ and $\Delta\omega_B = \omega_B - \omega_r$ are the frequency offsets for resonances of A and B. Similar equations hold for the B magnetization.

The Steady-State Saturation-Transfer Experiment

The longitudinal magnetization of A is measured at steady state in the presence of a RF field of frequency ω_B, which saturates the B magnetization. It is also measured in the presence of a RF field of the same amplitude and frequency ω_{sym}, defined as $\omega_{sym} - \omega_A = \omega_A - \omega_B$ (Fig. 1). The two measured values are called M_{sat}^A and M_{sym}^A respectively.

If the RF field applied at frequency ω_{sym} does not perturb the magnetization components of A and B, $M_{sym}^A = M_0^A$. In this case, M_{sat}^A differs from M_0^A only because B magnetization has a new steady-state value and because of chemical exchange between A and B. This can be determined via the Bloch equations (Eqs. [2] to [4]), in which M_z^B is set to 0 and the terms including ω_1 are neglected. This is a good assumption, as $\Delta\omega_A \gg \omega_1$. Then, M_x^A and M_y^A oscillate very rapidly and the average contribution of $\omega_1 M_y^A$ to M_z^A can be neglected. The magnetization of A at steady state is deduced solely from Eq. [4] and is $M_{sat}^A = M_0^A \tau_{1A}/T_{1A}$. The saturation-transfer ratio $R_A = M_{sat}^A/M_{sym}^A$ is then equal to τ_{1A}/T_{1A} in the absence of spill-over.

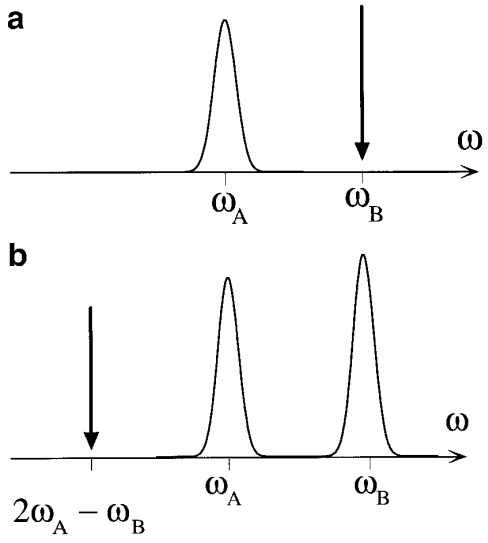

FIG. 1. For two nuclei A and B in chemical exchange, observation of A longitudinal magnetization when the low power RF field is applied at the angular frequency ω_B (a), and $\omega_{sym} = 2\omega_B - \omega_A$ (b).

Existence of a Spill-over Effect

Spill-over may occur if the chemical shift between A and B is small, or if the intensity of the RF saturating field is large. The magnetization of A at steady-state is attenuated by the low power RF field, whatever its frequency, ω_B or ω_{sym}.

At first glance, a RF field applied at frequency ω_B or ω_{sym} with the same symmetrical power envelope should cause the same attenuation in A magnetization if its lineshape is symmetrical. This is obviously true if there is no chemical exchange between populations A and B. However, during the control experiment, the spill-over upon A, and eventually B, modifies A magnetization at steady state in a different way than when B magnetization is kept continuously saturated: this attenuation is shared between A and B, because of chemical exchange. The exact values of M_{sat}^A and M_{sym}^A can be calculated by solving the system of Eqs. [2] to [4] at steady state. But, contrary to the previous situation, the terms containing the ω_1 factor in these equations can no longer be neglected. The six components M_x^A, M_y^A, M_z^A, M_x^B, M_y^B, and M_z^B are now interrelated and the magnetization values M_{sat}^A and M_{sym}^A cannot be deduced from simple formulas.

New Basis Set

The use of co-ordinates linked to each of the effective magnetic fields at A and B (*17, 18*) makes easier the analysis of

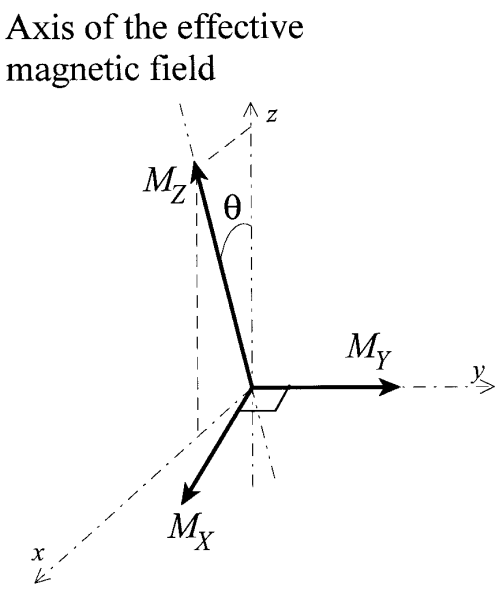

FIG. 2. Decomposition of a magnetization in the new basis (X, Y, Z) linked to its effective magnetic field. The axes x, y, and z correspond to the frame rotating at the angular frequency ω_r of B_1. Z is aligned along the effective magnetic field. The angle between z and Z axis is called θ.

their magnetization behavior. With this procedure, nonsecular contributions can be eliminated and the values of A and B magnetization components can be calculated. In the frame rotating at frequency ω_r, we define for each population the new axes $\{X, Y, Z\}$, as represented in Fig. 2. Although they have the same names, the axes X, Y, and Z correspond to different orientations for A and B. For a given population, the Z axis is aligned with the effective field, given by the relation

$$\mathbf{B}_{\text{eff}}^{\text{A}} = -\frac{\omega_{\text{A}} - \omega_{\text{r}}}{\gamma}\mathbf{e}_z - \frac{\omega_1}{\gamma}\mathbf{e}_x = -\frac{\mathbf{\Omega}_{\text{A}}}{\gamma}$$

for A and the same for B. Ω_{A} and Ω_{B} are the precession angular frequencies of A and B's magnetization in the tilted frames. The magnetization of a given population has one component along the axis of the effective magnetic field, called M_Z, and two perpendicular components, called M_X and M_Y. The angle θ between the Z axis, parallel to its effective field, and the z axis, parallel to $\mathbf{B}_0$, can be deduced from

$$\tan\theta = \frac{\omega_1}{\Delta\omega}. \qquad [5]$$

The change of variables corresponds to a transformation in a doubly tilted single rotating frame. The equations of the time dependence of these components with chemical exchange have already been derived in this new basis set (*17*) and are

$$\frac{d}{dt}\begin{pmatrix} M_X^{\text{A}} \\ M_Y^{\text{A}} \\ M_Z^{\text{A}} \\ M_X^{\text{B}} \\ M_Y^{\text{B}} \\ M_Z^{\text{B}} \end{pmatrix} = \begin{pmatrix} \mathsf{S}_{\text{A}} & \mathsf{T}_{\text{B}} \\ \mathsf{T}_{\text{A}} & \mathsf{S}_{\text{B}} \end{pmatrix} \times \begin{pmatrix} M_X^{\text{A}} \\ M_Y^{\text{A}} \\ M_Z^{\text{A}} \\ M_X^{\text{B}} \\ M_Y^{\text{B}} \\ M_Z^{\text{B}} \end{pmatrix} + \begin{pmatrix} -(M_0^{\text{A}}/T_{1\text{A}})\sin\theta_{\text{A}} \\ 0 \\ (M_0^{\text{A}}/T_{1\text{A}})\cos\theta_{\text{A}} \\ -(M_0^{\text{B}}/T_{1\text{B}})\sin\theta_{\text{B}} \\ 0 \\ (M_0^{\text{B}}/T_{1\text{B}})\cos\theta_{\text{B}} \end{pmatrix} \qquad [6]$$

with

$$\mathsf{S}_{\text{A}} = \begin{pmatrix} -\left(\frac{\sin^2\theta_{\text{A}}}{\tau_{1\text{A}}} + \frac{\cos^2\theta_{\text{A}}}{\tau_{2\text{A}}}\right) & -\Omega_{\text{A}} & \sin\theta_{\text{A}}\cos\theta_{\text{A}}\left(\frac{1}{\tau_{1\text{A}}} - \frac{1}{\tau_{2\text{A}}}\right) \\ \Omega_{\text{A}} & -\frac{1}{\tau_{2\text{A}}} & 0 \\ \sin\theta_{\text{A}}\cos\theta_{\text{A}}\left(\frac{1}{\tau_{1\text{A}}} - \frac{1}{\tau_{2\text{A}}}\right) & 0 & -\left(\frac{\sin^2\theta_{\text{A}}}{\tau_{2\text{A}}} + \frac{\cos^2\theta_{\text{A}}}{\tau_{1\text{A}}}\right) \end{pmatrix}$$

$$\mathsf{T}_{\text{A}} = \frac{1}{\tau_{\text{A}}}\begin{pmatrix} \cos(\theta_{\text{A}} - \theta_{\text{B}}) & 0 & \sin(\theta_{\text{A}} - \theta_{\text{B}}) \\ 0 & 1 & 0 \\ -\sin(\theta_{\text{A}} - \theta_{\text{B}}) & 0 & \cos(\theta_{\text{A}} - \theta_{\text{B}}) \end{pmatrix}$$

and the symmetrical matrices for S_{B} and T_{B}. These equations can be simplified more easily than those written in the nontilted frame, as will now be shown.

Approximations

When the low power RF field is continuously applied at frequency ω_{B},

$$|\Delta\omega_{\text{A}}| = |\omega_{\text{A}} - \omega_{\text{B}}| \gg \frac{1}{\tau_{2\text{A,B}}},$$

as the peaks of A and B do not overlap. On the other hand, the inequalities

$$\frac{1}{\tau_{2A}} \geqslant \frac{1}{\tau_{1A}}, \frac{1}{\tau_A} \quad \text{and} \quad \frac{1}{\tau_{2B}} \geqslant \frac{1}{\tau_{1B}}, \frac{1}{\tau_B} \qquad [7]$$

always hold, as chemical exchange is slow. Moreover, $|\Omega_A| = \sqrt{(\Delta\omega_A)^2 + (\omega_1)^2}$. Therefore,

$$|\Omega_A| \gg \frac{1}{\tau_{2A,B}}, \frac{1}{\tau_{1A,B}}, \text{ and } \frac{1}{\tau_{A,B}}. \qquad [8]$$

When the RF field is applied at ω_{sym}, the frequency offsets $|\Delta\omega_A|$ and $|\Delta\omega_B|$ are respectively equal to $|\omega_A - \omega_B|$ and $2|\omega_A - \omega_B|$. As previously for A, the precession angular frequencies of A and B hold:

$$|\Omega_{A,B}| \gg \frac{1}{\tau_{2A,B}}, \frac{1}{\tau_{1A,B}}, \text{ and } \frac{1}{\tau_{A,B}}. \qquad [9]$$

Thus, the magnetization components along X and Y of A or B off-resonance oscillate and are zero at steady state, as the magnetization is then aligned to its effective magnetic field (*19*). Moreover, the low power RF field continuously applied at frequency ω_B is strong enough to saturate B magnetization. So, the components M_X^B and M_Y^B are equal to nil at steady state. Finally, for $\omega_r = \omega_B$ or ω_{sym}, M_X^A, M_Y^A, M_X^B, and M_Y^B are equal to zero at steady state.

The system of Eq. [6] can then be simplified. The values of M_Z^A and M_Z^B at steady state are solutions of the simultaneous equations

$$-\left(\frac{\cos^2\theta_A}{\tau_{1A}} + \frac{\sin^2\theta_A}{\tau_{2A}}\right) M_{Zeq}^A + \frac{\cos(\theta_A - \theta_B)}{\tau_B} M_{Zeq}^B + \frac{\cos\theta_A}{T_{1A}} M_0^A = 0 \qquad [10]$$

$$-\left(\frac{\cos^2\theta_B}{\tau_{1B}} + \frac{\sin^2\theta_B}{\tau_{2B}}\right) M_{Zeq}^B + \frac{\cos(\theta_A - \theta_B)}{\tau_A} M_{Zeq}^A + \frac{\cos\theta_B}{T_{1B}} M_0^B = 0. \qquad [11]$$

The Value of A Magnetization

The system of Eqs. [10] and [11] is more easily solved than the system of Bloch equations in the rotating frame. It is now possible to determine analytically the value of A magnetization at steady state, which is

$$M_{Zeq}^A = \frac{(\cos\theta_A/T_{1A}\tau_{ZB}) + \cos\theta_B\cos(\theta_A - \theta_B)/T_{1B}\tau_A}{(1/\tau_{ZA}\tau_{ZB}) - \cos^2(\theta_A - \theta_B)/\tau_A\tau_B} M_0^A \qquad [12]$$

with

$$\frac{1}{\tau_{ZA}} = \frac{\cos^2\theta_A}{\tau_{1A}} + \frac{\sin^2\theta_A}{\tau_{2A}} \quad \text{and} \quad \frac{1}{\tau_{ZB}} = \frac{\cos^2\theta_B}{\tau_{1B}} + \frac{\sin^2\theta_B}{\tau_{2B}}.$$

The longitudinal magnetization of A is the value of interest during saturation-transfer experiments. It is given by the relation

$$M_{zeq}^A = \cos\theta_A \cdot M_{Zeq}^A = \cos\theta_A \times \frac{(\cos\theta_A/T_{1A}\tau_{ZB}) + \cos\theta_B\cos(\theta_A - \theta_B)/T_{1B}\tau_A}{(1/\tau_{ZA}\tau_{ZB}) - \cos^2(\theta_A - \theta_B)/\tau_A\tau_B} M_0^A. \qquad [13]$$

It is equal to M_{sat}^A when the continuous RF field is applied at ω_B and M_{sym}^A when the field is applied at ω_{sym}. To determine its value, it is useful to look at the geometry of the system represented in Fig. 3, where B_{eff}^A and B_{eff}^B are drawn for $\omega_r = \omega_B$ (a) and ω_{sym} (b). When the RF field is applied at ω_B, $\theta_B = \pi/2$, $M_{zeq}^A \equiv M_{sat}^A$. In this case, Eq. [13] can be simplified and become

$$M_{sat}^A = \frac{\cos^2\theta_A/T_{1A}}{(1/\tau_{ZA}) - (\tau_{2B}/\tau_A\tau_B)\sin^2\theta_A} M_0^A. \qquad [14]$$

When the RF field is applied at ω_{sym}, θ_A is replaced by $\theta'_A = \pi - \theta_A$ and θ'_B is given by the relation: $\tan\theta'_B = \tan(\theta'_A)/2$. Equation [13] is unchanged if θ_A and θ_B are replaced by $\pi - \theta_A$ and $\pi - \theta_B$ respectively. So, for a given angle θ_A, M_{sym}^A is equal to M_{Zeq}^A of Eq. [13], if θ_B obeys the relation

$$\tan\theta_B = \frac{\tan\theta_A}{2}. \qquad [15]$$

The Saturation-Transfer Ratio

The ratio $R_A = M_{sat}^A/M_{sym}^A$ is deduced from Eqs. [13] and [14]

$$R_A = \frac{(\cos\theta_A/T_{1A})((1/\tau_{ZA}\tau_{ZB}) - (\cos^2(\theta_A - \theta_B)/\tau_A\tau_B))}{((1/\tau_{ZA}) - (\tau_{2B}/\tau_A\tau_B)\sin^2\theta_A)((\cos\theta_A/T_{1A}\tau_{ZB}) + (\cos\theta_B\cos(\theta_A - \theta_B)/T_{1B}\tau_A))} \qquad [16]$$

with θ_B defined by Eq. [15].

This ratio can be studied as a function of θ_A for a given set of relaxation and exchange parameters. It is calculated here for a two-spin system having the same relaxation time values for both spins ($T_1 = 6$ s, $T_2 = 2$ s) and equal magnetization values at equilibrium. Different chemical-exchange rates

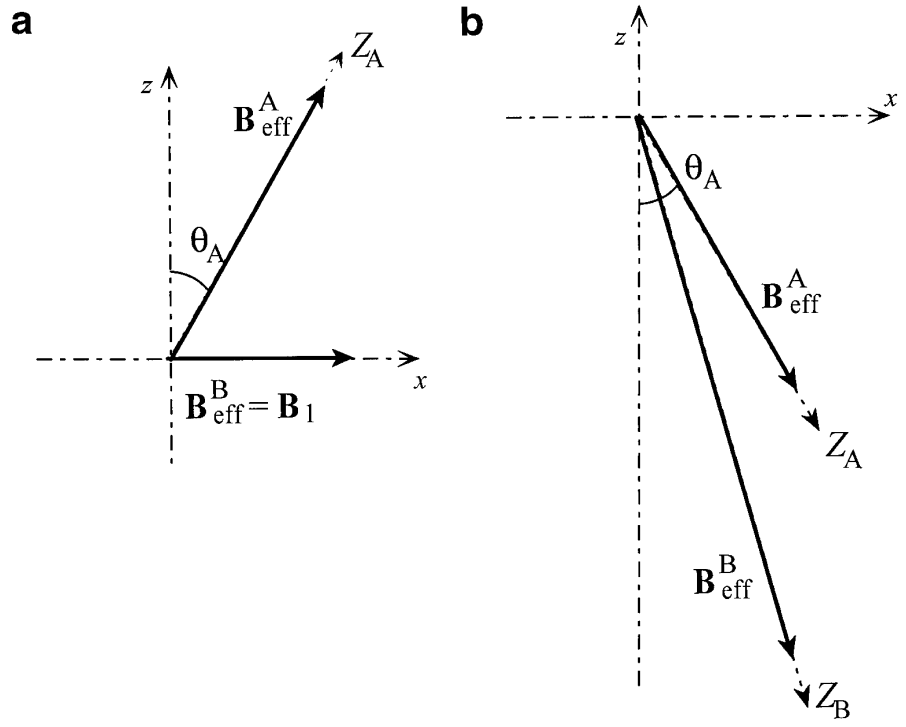

FIG. 3. Effective magnetic fields of the exchanging nuclei A and B in the rotating frame when the low-power RF field is applied at the angular frequency ω_B (a) and ω_{sym} (b). B^A_{eff} and B^B_{eff} are the effective magnetic fields of A and B respectively; they represent the orientations of M^A_Z and M^B_Z.

are used ($\tau_1/T_1 = 0.2$, 0.3, and 0.7), and it is assumed that B magnetization is totally saturated when it is on resonance. The results are shown in Fig. 4. In some spin systems, $\omega_A - \omega_B$ is small and/or a large RF field is necessary to saturate completely B magnetization. In this case, it may be impossible to saturate B and keep the angle θ_A close to zero. Hence, the beginning of this curve cannot be obtained experimentally. The saturation-transfer ratio at $\theta_A = 0$ represents an hypothetical value bound to the absence of any spill-over.

From the curves drawn in Fig. 4, one observes that, as θ_A increases, the ratio R_A differs from the expected value τ_1/T_1. This means that the spill-over effect is not the same on M^A_{sat} and M^A_{sym}. Thus, the application of a low-power RF field at the frequency ω_{sym} during the acquisition of the reference spectrum does not suppress the artifact on R_A due to spill-over.

EXPERIMENTAL

The theoretical prediction illustrated in Fig. 4 was verified experimentally with *N,N*-dimethylacetamide in aqueous solution. The hindered internal rotation of this molecule about the C–N bond provides an exchange mechanism for the two *N*-methyl groups. This dynamic process studied by proton NMR at 11.4 T is slow up to 100°C (*20*).

N,N-Dimethylacetamide, obtained from Sigma, was diluted at 10% (v/v) in deuterated water and analyzed at 50°C in a 5-mm sample tube. Proton NMR spectra were obtained at 500 MHz using a Bruker DRX500 spectrometer and a 5-mm proton probe. They are composed of three peaks, the relative frequencies of which are given in Table 1. The *b* peak at 4.07 ppm and the *a* peak at 3.91 ppm are assigned to the protons of the exchanging *N*-methyl groups.

Each saturation-transfer single experiment included two measurements of the *a* longitudinal magnetization at steady state in the presence of a low-power RF field applied at two different frequencies. This field was applied continuously during 35 s on the transmitter channel before each measurement. This is long enough for the monitored magnetization to reach a steady state. Then, a high power $\pi/2$ read pulse was applied to rotate the longitudinal magnetization into the transverse plane. Phase cycling was used to prevent the recording of undesired transverse components. The spectral width was the same for the two measurements. The measured intensity of *a* magnetization was called M^a_{sat} when the frequency of the low-power RF field was ω_b, and M^a_{sym} when its frequency was $\omega_{sym} = 2\omega_a - \omega_b$. This experiment was repeated for different amplitudes of the saturating field. The FIDs were averaged over 32 scans with 8 K points. Exponential apodization (0.5 Hz line broadening) was performed prior to Fourier transformation. The phase and baseline of the spectra were corrected manually. The resonance intensities were measured via the peak areas. The amplitude of the low-power RF field, which is proportional to ω_1, was defined in frequency units and deduced from the length of the $\pi/2$ soft pulse. For an easier comparison with theoretical results, the angle between the effective field related to *a* and the *z* axis,

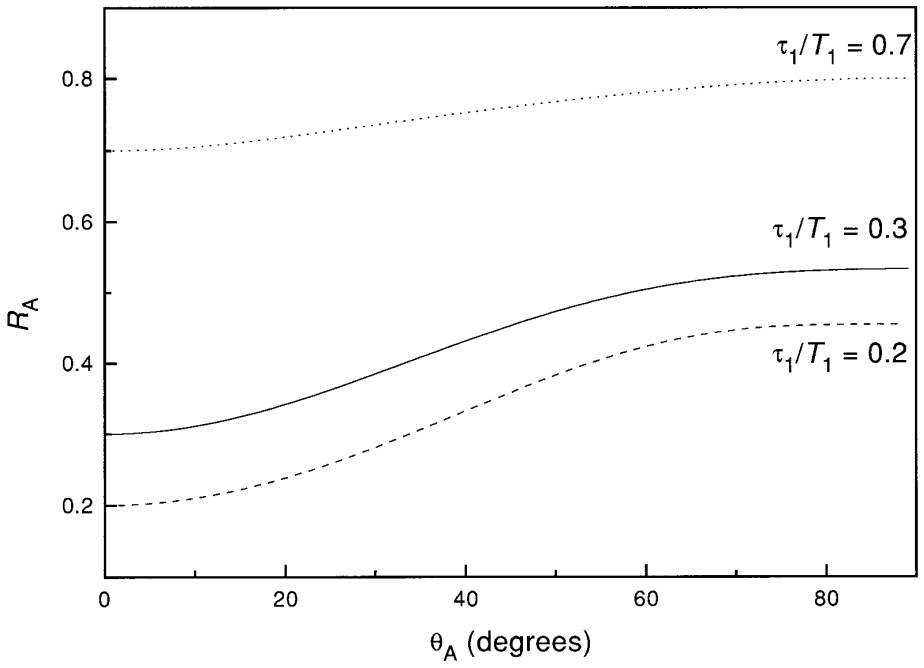

FIG. 4. Theoretical evolution of the ratio $R_A = M^A_{sat}/M^A_{sym}$ as a function of the angle θ_A between the A effective magnetic field and the z axis in the rotating frame. It is assumed that A and B magnetization components have equal relaxation times, $T_1 = 6$ s, $T_2 = 2$ s, and equal intensities at thermodynamic equilibrium. Different chemical exchange rates are considered: $\tau_1/T_1 = 0.7$, $\tau_1/T_1 = 0.3$, and $\tau_1/T_1 = 0.2$.

$$\theta = \arctan\left|\frac{\omega_1}{\omega_a - \omega_b}\right|,$$

was chosen to express the amplitude of the saturating field.

The measured intensities, M^a_{sat} and M^a_{sym}, are represented in Fig. 5a. As expected, they decrease when the saturating field amplitude increases. The variations of the ratio $R_a = M^a_{sat}/M^a_{sym}$ as a function of the angle θ are shown in Fig. 5b. In both figures, the dotted and dashed lines represent the best fit of the experimental points using Eqs. [13], [14], and [16], which was found in the following way: it was assumed that the magnetization components of *a* and *b* have the same relaxation times, and are of equal value at thermodynamic equilibrium. The relaxation time constant τ_{1a}, measured separately at 50°C, $B_0 = 11.7$ T, by studying the time course of *a* longitudinal magnetization while *b* is selectively saturated without any spill-over effect on *a*, was set to 1.46 s. The two other parameters τ ($=\tau_a = \tau_b$) and τ_2 ($=\tau_{2a} = \tau_{2b}$) were adjusted to fit the experimental data. Their values are given in the legend of Fig. 5.

TABLE 1
^{1}H Resonance Frequencies at 11.7 T and 50°C of N,N-Dimethylacetamide Diluted at 10% v/v in D_2O

	Frequency	
Peak	(Hz)	(ppm)
b	2033.25	4.07
a	1955.86	3.91
c	1544.70	3.09

Note. Values were obtained by setting water resonance at 4.75 ppm. The *a* and *b* resonances correspond to the protons in chemical exchange.

The theoretical curves are found not to fit the experimental results when $\theta \geqslant 60°$. For a better understanding of the difference observed, similar saturation-transfer experiments were done by measuring the longitudinal magnetization of *b*. The two RF frequencies were then ω_a and $2\omega_b - \omega_a$; the saturation-transfer ratio which was measured, R_b, is represented with R_a in Fig. 6a. The theoretical curves were fitted to the experimental data as before in Fig. 5, except that the equality of *a* and *b*'s relaxation times was no longer assumed. Globally, the experimental results confirm the main theoretical conclusion which is a marked increase of the ratios R_a and R_b when the amplitude of the low-power RF field becomes large. The theoretical curves are in good agreement with the experimental data up to the angle $\theta = 60°$. It is interesting to note that for θ values larger than 60°, R_a and R_b evolve differently on the two sides of the theoretical curves. The difference between theory and experiment is not due to a lack of precision in the measurements, as these results are quite reproducible. It cannot be explained by differences between *a* and *b* relaxation times either.

So, to improve the fit for $\theta \geqslant 60°$, the dipolar couplings between *b* and the two other methyl groups, *a* and *c*, were

taken into account. These dipolar couplings may induce detectable changes on a and b's magnetization for large ω_1 values, when the saturating field employed is strong enough to saturate partially c. This partial saturation depends on the RF field frequency: it is more important when M_a^{sym} and M_b^{sat} are measured. Then, these values are more increased by dipolar couplings than M_a^{sat} and M_b^{sym}. As a consequence, R_b is increased and R_a decreased. The dipolar coupling constant between the protons of b and c along the z axis, σ_{bc}, and the relaxation times of c along the z axis and in the rotating frame T_{1c} and T_{2c} were measured. The average distances between the protons of the methyl groups were calculated with the program Hyperchem. The dipolar coupling constants along the z axis, σ_{ab}, and in the rotating frame, μ_{ab} and μ_{bc}, were then calculated in the extreme-narrowing limit ($\omega_0\tau_c \ll 1$). Dipolar couplings between a and b, on one hand, and b and c on the other were included in our model to determine the saturation-transfer ratios R_a and R_b. The equations employed are given in the Appendix. The adjusted curves are shown in Fig. 6b. They correspond quite well to experimental data for R_a but not for R_b. The inability to fit simultaneously the two curves may be explained in different ways: a poor choice of the values of some of the unknown parameters, or the existence of a small J coupling between the methyl groups a and c, for example. However, it is interesting to note that the existence of dipolar couplings between the methyl groups modifies the value of R_a in the same way as that which is observed experimentally.

To summarize, the difference between theory and experiment for $\theta > 60°$ arises from the structure of *N,N*-dimethylacetamide which is not exactly a two-spin system. It is not

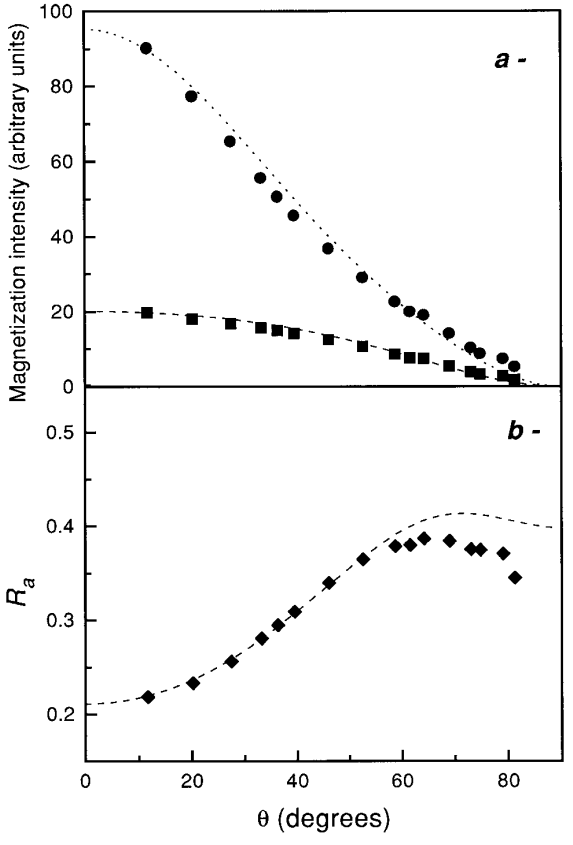

FIG. 5. Study of the spill-over as a function of the RF field magnitude during saturation-transfer experiments. *N,N*-Dimethylacetamide 10% v/v, at 50°C; $B_0 = 11.7$ T. The magnitude of the RF field is characterized by the angle θ between the a effective magnetic field and the z axis. (a) The longitudinal magnetization of a is measured while b is saturated (■) and when a RF field with frequency $\omega_{\mathrm{sym}} = 2\omega_a - \omega_b$ is applied (●). The measured values are called M^a_{sat} and M^a_{sym} respectively. (b) Values of the saturation-transfer ratio $R_a = M^a_{\mathrm{sat}}/M^a_{\mathrm{sym}}$ deduced from the above measurements (♦). The curves drawn in (a) and (b) represent the best fit of the experimental data for a two-spin system model. Two independent parameters, τ_a and τ_{2a}, are adjusted. The parameters of the fitting curves are $\tau_{1a} = \tau_{1b} = 1.46$ s, $\tau_{2a} = \tau_{2b} = 1.4$ s, and $\tau_a = \tau_b = 1.85$ s.

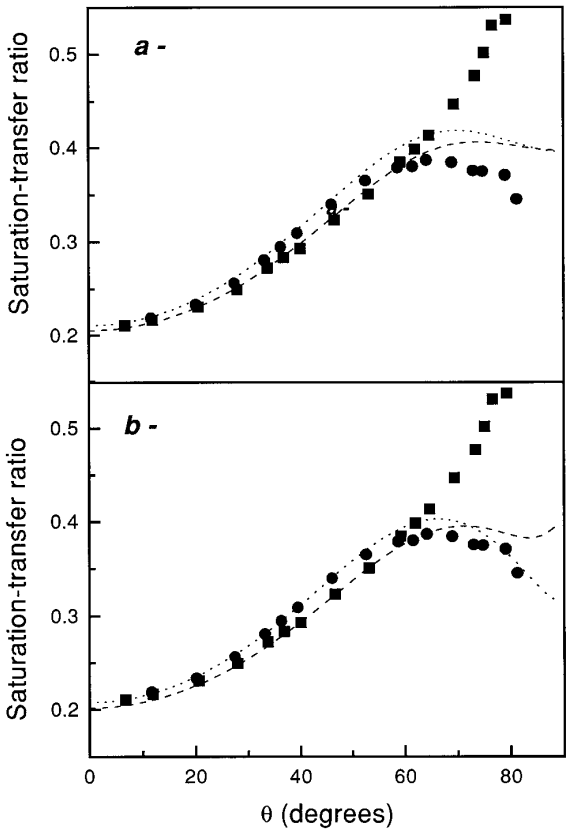

FIG. 6. Saturation transfer at steady state with *N,N*-dimethylacetamide at 50°C, $B_0 = 11.7$ T. Both the ratios R_a (●) and R_b (■) are now measured. The curves represent the best fit to the experimental points via different models, . . . for R_a and --- for R_b. (a) The model chosen is a two-spin system with a and b in chemical exchange. The parameters of these curves are $\tau_{1a} = 1.47$ s, $\tau_{1b} = 1.46$ s, $\tau_{2a} = 1.46$ s, $\tau_{2b} = 1.35$ s, $\tau_a = \tau_b = 1.85$ s. τ_a and τ_b only, are assumed to be equal. (b) The dipolar couplings between a and b, on one hand, and b and c on the other are taken into account in the theoretical values of R_a and R_b. $T_{1c} = 7.73$ s and $\sigma_{bc} = 0.0063$ were measured in another experiment. $\mu_{bc} = 0.004$, $\sigma_{ab} = 0.016$, $\mu_{ab} = 0.01$ are deduced from the σ_{bc} value. The other values of τ_{1a}, τ_{1b}, τ_{2a}, and τ_{2b} are chosen as in (a). The best value of τ_a and τ_b to fit the experimental values is 1.79 s.

due to a failure of our model to describe such a system. Another two-spin system in chemical exchange, without scalar nor dipolar couplings, would be an interesting alternative to test the model.

DISCUSSION

These results show that the off-resonance irradiation may cause a systematic error during saturation-transfer measurements at steady state, even if a contralateral irradiation is used during the reference measurement. The attenuations of the monitored A magnetization by the off-resonance irradiation during saturation of B magnetization and during the usual ''symmetrical'' irradiation are different. The use of co-ordinates linked to the effective magnetic fields of A and B is useful for determining the spill-over magnitude on the saturation-transfer ratio.

It is only when chemical exchange occurs between A and B that the spill-over effect on A is different if the RF field is applied at ω_B or at ω_{sym}. Consequently, the measurement of a saturation-transfer ratio $R_A < 1$ means unambiguously that the populations A and B are in chemical exchange. Hence, recording the reference spectrum with a ''symmetrical'' irradiation is useful for checking the existence of a chemical-exchange process. Moreover, the equality of A magnetization values at steady state when the RF field is applied at ω_{sym} and far away off-resonance ensures the absence of any spill-over effect. In this case, it is possible to deduce the rate of chemical exchange from the standard saturation-transfer experiment (*1, 2*).

Elsewhere, the magnitude of the spill-over effect may be determined via the model presented here. This can be done in two different ways. Until $\theta_A = 30°$, the spill-over effect is not very important and it can be calculated approximately: it is possible to develop R_A of Eq. [16] to the second order of θ_A. It is equal to

$$R_A = \frac{\tau_{1A}}{T_{1A}}\left[1 + \frac{\theta_A^2}{\tau_A}\frac{K_1}{K_2}\right] \qquad [17]$$

with θ_A in radians and

$$K_1 = -\frac{1}{2\tau_B} + \frac{1}{4\tau_{2B}} - \frac{1}{2\tau_{1B}} + \frac{\tau_{1A}}{\tau_{2A}\tau_B} + \frac{\tau_{2B}}{\tau_{1B}\tau_B} - \frac{\tau_{1A}\tau_{2B}}{\tau_A\tau_B^2} \qquad [18]$$

$$K_2 = \frac{1}{\tau_{1A}\tau_{1B}} - \frac{1}{\tau_A\tau_B}. \qquad [19]$$

Then, for a given saturation-transfer experiment, it is possible to estimate the magnitude of spill-over and determine τ_{1A}/T_{1A} (Fig. 7). For that, the measured values of the relaxation and chemical-exchange rates should be input in the terms multiplied by θ_A^2. Under these conditions, the systematic errors on the parameters due to spill-over can be neglected. If one wants to deduce the rate of chemical exchange from this saturation-transfer measurement, one should also measure precisely the longitudinal relaxation rate of A, T_{1A}, while the exchange between A and B is stopped. This can be done in some biological systems where the desired biochemical reaction is stopped (*15*), but it may be impossible to do so in other systems.

For larger values of θ_A, another method should be employed. Several saturation-transfer experiments at steady state should be carried out for different intensities of the saturating field and the expected parameters obtained via curve fitting. If other nuclei interact with A and B, even weakly, one should be careful about the spill-over effect on these nuclei when using strong RF fields. This second-rank off-resonance effect could change the saturation-transfer ratio in a nonnegligible manner. If one wants to obtain precise results, it is better to know some of the relaxation times of the exchanging populations A and B and to input their values in the model as constant parameters before fitting the curves to the saturation-transfer experimental data.

The easier two-spin system to study is one where A and B have the same exchange rates and relaxation times. As the fitting curves depend on three parameters, τ, τ_1, and τ_2, it is sufficient to measure one relaxation time of A or B and the saturation-transfer ratio for one population. If one needs to determine the transverse relaxation time, one may use either the Hahn-echo, CPMG, or spin-lock sequences; these two last sequences lead to the intrinsic relaxation times T_{2A} and T_{2B} if the magnetization components of A and B are equal at the beginning of the evolution time, even in the presence of J couplings or diffusion. The relaxation-time measurements are more difficult when A and B have different properties. When the CPMG and spin-lock sequences are used, the exchanging transverse magnetizations are aligned during the evolution time. The transverse magnetization of each exchanging population generally does not evolve monoexponentially, which makes it difficult to determine the transverse relaxation times. These times can be determined via a spin-echo pulse sequence, as chemical exchange is slow. This measurement gives rise to τ_{2A} and τ_{2B}, although it may be difficult to determine these relaxation times precisely in the presence of small J couplings. It may also be difficult to measure the longitudinal relaxation-time values: the experimental values of τ_{1A} and τ_{1B} may be modified by spill-over. If possible, one should measure the relaxation times T_{1A} and T_{1B} while the exchange between A and B is stopped. Additionally, the saturation-transfer ratios should be measured for both A and B.

Whatever the spin-system, where A and B have similar or different relaxation properties, the chemical-exchange rates are deduced from the parameters of the curves fitted to the satura-

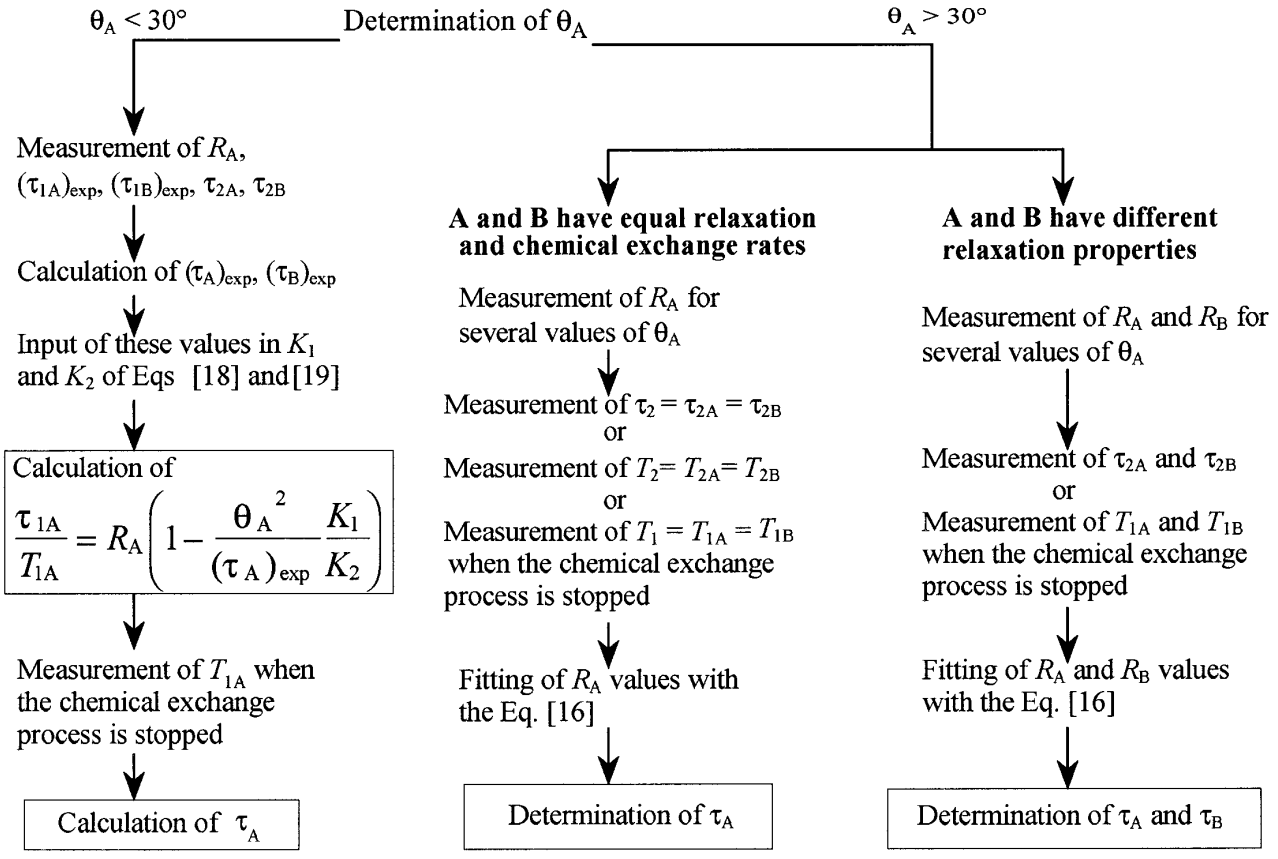

FIG. 7. Flow chart useful to study the chemical exchange between A and B using saturation transfer and to determine the chemical-exchange rate constants in the presence of a spill-over effect. When $\theta_A < 30°$, an approximate value of the saturation-transfer ratio without any spill-over artifact can be calculated. For that, the relaxation times are measured and the chemical-exchange rate constants calculated despite the spill-over. They are then put in a formula to determine an approximate value of τ_{1A}/T_{1A}. This value also permits the determination of the chemical-exchange rate if T_{1A} can be measured. When $\theta_A > 30°$, the experimental values of R_A and R_B as a function of θ_A are fitted by a theoretical model. The parameters of the fitted curves give the rate of chemical exchange.

tion-transfer results. The experiment is more time consuming and the analysis more difficult when A and B have different relaxation properties. It may be then more interesting to employ other magnetization-transfer experiments than saturation-transfer to determine the rate of chemical exchange if spill-over occurs. But, in both cases, the method described above could be used, and gives significant results, if one wants to study very precisely a spin system and check the absence of interactions with other nuclei. In the present case, the divergence between experiment and theory for saturation-transfer experiments with large RF fields showed that *N,N*-dimethylacetamide is not exactly a two-spin system in chemical exchange. Taking into account the dipolar couplings between the methyl groups of *N,N*-dimethylacetamide changes the chemical-exchange value, deduced from the fitting curves of *a* and *b* resonances, by about 3%. A study is under way to determine how *J* couplings may modify the saturation-transfer ratio for large RF field intensities and to find a good theoretical model for systems as *N,N*-dimethylacetamide at larger saturating-field magnitudes.

Practically, the amplitude of the saturating field is in most cases very low and/or the chemical shift between the resonance frequencies of the exchanging nuclei is quite large. Under these conditions, the angle between the effective magnetic field of the monitored magnetization A and the static magnetic field B_0 is very small and the spill-over effect can be neglected. For example, during the measurement of phosphorus exchange between inorganic phosphate and ATP in living plant tissues at 9.4 T, the offset $\omega_A - \omega_B$ and the amplitude of the saturating RF field are such that $\theta_A = 1°$. Then, the contralateral irradiation at ω_{sym} does not produce spill-over. The rate of ATP synthesis can be determined directly from the saturation-transfer experiment. This should also apply for the reaction between γATP and creatine phosphate in animal cells where, using the same ω_1 value, the angle θ_A would be 3°. At a matter of fact, it has been found that, for the study of the myocardial creatine-kinase reaction, the off-resonance effect on the creatine phosphate was about 10% when irradiating the P_i peak (*21*). This would mean that the angle θ_A was then larger than 10°. This confirms that the condition of saturation depends sharply on the experimental setup and on the sample actually studied.

The usual way to avoid the spill-over effect upon the saturation-transfer ratio is to choose the magnitude of the RF field to be as small as possible. But one should be careful to saturate totally the magnetization B on resonance. Otherwise, another artifact will appear on R_A, which could be larger than that avoided. Whereas this artifact is usually easily corrected, this is no longer possible if imperfect saturation and spill-over occur simultaneously. In this case, it is better to use a RF field large enough to saturate the magnetization on resonance. In most spin-systems, the angle θ_A will still be smaller than 30° and the spill-over effect on the saturation-transfer ratio can be determined directly.

CONCLUSION

It has been shown that even the robust saturation-transfer method is only valid up to a certain point if an accurate result is required. The present work could serve as a guideline in deciding whether a saturation-transfer experiment yields a qualitative or an accurate quantitative result. A model has been developed to determine the rate of chemical exchange when no other technique than saturation-transfer can be used. It has been presented in reference to chemical exchange but dipolar coupling can be treated in a similar way if one keeps in mind that the rate of cross-relaxation is different along the z axis and in the perpendicular plane. The equations are then slightly different. They are given in the Appendix.

It is possible to describe much more complicated spin-systems in the same way. A three-spin system has been described in the presence of both chemical exchange and dipolar coupling as an example (see Appendix).

To conclude, the present approach can be applied in the many different fields where chemical exchange and dipolar couplings are present: cell metabolism or molecular structure, for example. It allows accurate measurements to be obtained when the objective is to look for the precise molecular mechanisms involved.

APPENDIX

Analysis of the N,N-Dimethylacetamide as a Three-Spin System with Chemical Exchange and Dipolar Couplings

In order to study more precisely *N,N*-dimethylacetamide, we consider the case where three spins interact. A and B are in chemical exchange, of which the rate is characterized by the same parameters as previously. There are also dipolar couplings between A and B, and between B and C. The rates of cross relaxation between A and B are called σ_{AB} and μ_{AB}. In the same way, they are called σ_{BC} and μ_{BC} between B and C. σ_{ij} refers to cross relaxation along the z axis, whereas μ_{ij} refers to cross relaxation in the transverse plane. It is assumed that $\sigma_{ij} = \sigma_{ji}$, $\mu_{ij} = \mu_{ji}$, which is true when $M_0^i = M_0^j$, as for *N,N*-dimethylacetamide. When no RF field is applied, the time course of A, B, and C magnetization is

$$\frac{d}{dt}M_z^A = -\frac{(M_z^A - M_0^A)}{T_{1A}} - \frac{M_z^A}{\tau_A} + \frac{M_z^B}{\tau_B} - (M_z^B - M_0^B)\sigma_{AB} \quad [20]$$

$$\frac{d}{dt}M_z^B = -\frac{(M_z^B - M_0^B)}{T_{1B}} - \frac{M_z^B}{\tau_B} + \frac{M_z^A}{\tau_A} - (M_z^A - M_0^A)\sigma_{AB} - (M_z^C - M_0^C)\sigma_{BC} \quad [21]$$

$$\frac{d}{dt}M_z^C = -\frac{(M_z^C - M_0^C)}{T_{1C}} - (M_z^B - M_0^B)\sigma_{BC} \quad [22]$$

along the z axis, and

$$\frac{d}{dt}M_+^A = -\frac{M_+^A}{T_{2A}} - \frac{M_+^A}{\tau_A} + \frac{M_+^B}{\tau_B} - M_+^B\mu_{AB} + \text{oscillating terms} \quad [23]$$

$$\frac{d}{dt}M_+^B = -\frac{M_+^B}{T_{2B}} - \frac{M_+^B}{\tau_B} + \frac{M_+^A}{\tau_A} - M_+^A\mu_{AB} - M_+^C\mu_{BC} + \text{osc. terms} \quad [24]$$

$$\frac{d}{dt}M_+^C = -\frac{M_+^C}{T_{2C}} - M_+^B\mu_{BC} + \text{osc. terms} \quad [25]$$

in the perpendicular plane.

The continuous low power RF field applied changes the magnetization orientation at steady state, which, for the population i, becomes tilted from the z axis with an angle $\theta_i = \arctan(\omega_1/\Delta\omega_i)$. As for a two-spin system, it is rewarding to work in a tilted frame. For three interacting spins, a triple-tilted rotating frame is used. The base transformation can be written in the same way as in (*17*)

$$\begin{pmatrix} M_L^A \\ M_L^B \\ M_L^C \end{pmatrix} = \begin{pmatrix} \Theta_A & 0 & 0 \\ 0 & \Theta_B & 0 \\ 0 & 0 & \Theta_C \end{pmatrix} \begin{pmatrix} M_I^A \\ M_I^B \\ M_I^C \end{pmatrix}, \quad [26]$$

where M_L^i and M_I^i are vectors with three components along the axes X, Y, Z and x, y, z respectively; Θ_i is a 3×3 rotation matrix of angle θ_i. In this new frame, only the components along the Z axis are nonsecular for each nucleus. The magnetization transfer between the different components depends on their relative orientations. For two populations i and j, whose effective fields are tilted from the z axis with angles θ_i and θ_j, the effective cross-relaxation coefficient becomes

$$\lambda_{ij} = \cos\theta_i\cos\theta_j\sigma_{ij} + \sin\theta_i\sin\theta_j\mu_{ij}. \quad [27]$$

The time course of the magnetization for the three populations A, B, and C is then

$$\frac{d}{dt}M_Z^A = \cos\theta_A\left(\frac{M_0^A}{T_{1A}} + M_0^B\sigma_{AB}\right) - \frac{M_Z^A}{\tau_{ZA}} + \frac{\cos(\theta_A - \theta_B)}{\tau_B}M_Z^B - \lambda_{AB}M_Z^B \quad [28]$$

$$\frac{d}{dt}M_Z^B = \cos\theta_B\left(\frac{M_0^B}{T_{1B}} + M_0^A\sigma_{AB} + M_0^C\sigma_{BC}\right) - \frac{M_Z^B}{\tau_{ZB}} + \frac{\cos(\theta_A - \theta_B)}{\tau_A}M_Z^A - \lambda_{AB}M_Z^A - \lambda_{BC}M_Z^C \quad [29]$$

$$\frac{d}{dt}M_Z^C = \cos\theta_C\left(\frac{M_0^C}{T_{1C}} + M_0^B\sigma_{BC}\right) - \frac{M_Z^C}{T_{ZC}} - \lambda_{BC}M_Z^B, \quad [30]$$

where T_{ZC} is the intrinsic relaxation time of C along the Z axis:

$$\frac{1}{T_{ZC}} = \frac{\cos^2\theta_C}{T_{1C}} + \frac{\sin^2\theta_C}{T_{2C}}. \quad [31]$$

The magnetization value at steady state for each population is then

$$M_Z^A = \left(\frac{\cos(\theta_A - \theta_B)}{\tau_B} - \lambda_{AB}\right)\tau_{ZA}M_Z^B + \cos\theta_A\left(\frac{M_0^A}{T_{1A}} + M_0^B\sigma_{AB}\right)\tau_{ZA} \quad [32]$$

$$M_Z^B = \frac{N}{D} \quad [33]$$

$$M_Z^C = -\lambda_{BC}T_{ZC}M_Z^B + \cos\theta_C\left(\frac{M_0^C}{T_{1C}} + M_0^B\sigma_{BC}\right)T_{ZC} \quad [34]$$

with

$$N = \cos\theta_B\left(\frac{M_0^B}{T_{1B}} + M_0^A\sigma_{AB} + M_0^C\sigma_{BC}\right) - \cos\theta_C\left(\frac{M_0^C}{T_{1C}} + M_0^B\sigma_{BC}\right)\lambda_{BC}T_{ZC} + \cos\theta_A\left(\frac{M_0^A}{T_{1A}} + M_0^B\sigma_{AB}\right) \times \left(\frac{\cos(\theta_A - \theta_B)}{\tau_A} - \lambda_{AB}\right)\tau_{ZA} \quad [35]$$

and

$$D = \frac{1}{\tau_{ZB}} - \lambda_{BC}^2T_{ZC} - \left(\frac{\cos(\theta_A - \theta_B)}{\tau_A} - \lambda_{AB}\right) \times \left(\frac{\cos(\theta_A - \theta_B)}{\tau_B} - \lambda_{AB}\right)\tau_{ZA}. \quad [36]$$

The saturation-transfer ratio can be determined via Eqs. [32] to [36], although, as its exact formula is rather complicated, we have opted not to write it out in full.

The Magnetization-Transfer Ratio for Two Dipolar-Coupled Spins

In the same way as for chemical exchange, it is possible to determine the magnetization-transfer coefficient between two populations A and B only dipolar coupled together. The cross-relaxation coefficients are σ_{AB} and μ_{AB}. The time course of M_Z^A and M_Z^B in the tilted frame is

$$\frac{d}{dt}M_Z^A = \cos\theta_A\left(\frac{M_0^A}{T_{1A}} + M_0^B\sigma_{BA}\right) - \frac{M_Z^A}{T_{ZA}} - \lambda_{BA}M_Z^B \quad [37]$$

$$\frac{d}{dt}M_Z^B = \cos\theta_B\left(\frac{M_0^B}{T_{1B}} + M_0^A\sigma_{AB}\right) - \frac{M_Z^B}{T_{ZB}} - \lambda_{AB}M_Z^A, \quad [38]$$

where λ_{AB} is defined as in Eq. [27], and T_{ZA}, T_{ZB} are the intrinsic relaxation times of A and B along the Z axis, defined as in Eq. [31].

The magnetisation of A along the z axis is equal to

$$M_{sat}^A = \cos^2\theta_A T_{ZA}\left(\frac{M_0^A}{T_{1A}} + M_0^B\sigma_{BA}\right) \quad [39]$$

when the saturating RF field is applied at ω_B, whereas it is equal to

$$M_{sym}^A = \frac{\cos^2\theta_A T_{ZA}((M_0^A/T_{1A}) + M_0^B\sigma_{BA}) - \cos\theta_A\lambda_{BA}T_{ZB}\cos\theta_B((M_0^B/T_{1B}) + M_0^A\sigma_{AB})}{(1/T_{ZA}) - \lambda_{AB}\lambda_{BA}T_{ZB}} \quad [40]$$

when the RF field is applied at ω_{sym}. The magnetization-transfer coefficient due to dipolar coupling is then

$$R_{dip} = \frac{M_{sat}^A}{M_{sym}^A} = \frac{\cos\theta_A((M_0^A/T_{1A}) + M_0^B\sigma_{BA}) \times (1 - \lambda_{AB}\lambda_{BA}T_{ZA}T_{ZB})}{\cos\theta_A((M_0^A/T_{1A}) + M_0^B\sigma_{BA}) - \lambda_{BA}T_{ZB}\cos\theta_B((M_0^B/T_{1B}) + M_0^A\sigma_{AB})}$$

$$\text{with } \theta_B = \arctan\left(\frac{\tan\theta_A}{2}\right). \quad [41]$$

ACKNOWLEDGMENTS

E.B. enjoyed a grant from the Commissariat à l'Energie Atomique during part of this work. The authors are indebted to Drs. Lyndon Emsley and Albrecht Roscher for critical discussion of the original manuscript and thankful to the referee whose remarks have been very useful in preparing the final version of this article. Françoise Mabon and Michel Trierweiler are thanked for assistance with the NMR spectrometer and Professor Charles Tellier for his help in using modeling programs.

REFERENCES

1. S. Forsén and R. A. Hoffman, *J. Chem. Phys.* **39,** 2892 (1963).
2. S. Forsén and R. A. Hoffman, *J. Chem. Phys.* **40,** 1189 (1964).
3. I. D. Campbell, C. M. Dobson, R. G. Ratcliffe, and R. J. P. Williams, *J. Magn. Reson.* **29,** 397 (1978).
4. D. Neuhaus and M. P. Williamson, ''The Nuclear Overhauser Effect in Structural and Conformational Analysis,'' Chaps. 5, 10, VCH, New York (1989).
5. J. R. Alger and R. G. Shulman, *Quat. Rev. Biophys.* **17,** 83 (1984).
6. K. M. Brindle, *Prog. NMR Spectrosc.* **20,** 257 (1988).
7. P. W. Kuchel, *NMR Biomed.* **3,** 102 (1990).
8. W. Kuhn, W. Offermann, and D. Leibfritz, *J. Magn. Reson.* **68,** 193 (1986).
9. R. G. S. Spencer, A. Horská, J. A. Ferretti, and G. H. Weiss, *J. Magn. Reson. B* **101,** 294 (1993).
10. D. Gadian, G. K. Radda, T. R. Brown, E. M. Chance, M. J. Dawson, and D. R. Wilkie, *Biochem. J.* **194,** 215 (1981).
11. J. R. Alger, J. A. den Hollander, and R. G. Shulman, *Biochemistry* **21,** 2957 (1982).
12. J. K. M. Roberts, D. Wemmer, and O. Jardetzky, *Plant. Physiol.* **74,** 632 (1984).
13. G. Robinson, B. E. Chapman, and P. W. Kuchel, *Eur. J. Biochem.* **143,** 643 (1984).
14. P. S. Hsieh and R. S. Balaban, *Magn. Reson. Med.* **7,** 56 (1988).
15. J. R. Potts, K. Kirk, and P. W. Kuchel, *NMR Biomed.* **1,** 198 (1989).
16. H. M. McConnell, *J. Chem. Phys.* **28,** 430 (1958).
17. E. Baguet and C. Roby, *J. Magn. Reson. A* **108,** 189 (1994).
18. H. Desvaux, P. Berthault, N. Birlirakis, and M. Goldman, *J. Magn. Reson. A* **108,** 219 (1994).
19. R. R. Ernst, G. Bodenhausen, and A. Wokaun, ''Principles of Nuclear Magnetic Resonance in One and Two Dimensions,'' Chap. 4, Oxford Univ. Press, London (1987).
20. J. Jeener, B. H. Meier, P. Bachmann, and R. R. Ernst, *J. Chem. Phys.* **71,** 4546 (1979).
21. K. Ugurbil, M. Petein, R. Maidan, S. Michurski, and A. H. L. From, *Biochemistry* **25,** 100 (1986).